Journal of Physical Sciences, Vol. 25, 2020, 57-67
ISSN: 2350-0352 (print), www.vidyasagar.ac.in/publication/journal
Published on 16 October 2020

Synthesis and Magnetic studies of Co-Sn doped Nanoscale Calcium Hexaferrites

N. N Sarkar[1], D. J Roy[2], S.M Butte[3], W.S Barde[4] and K.G Rewatkar[5]

[1,3,4]Department of Physics, Shri Shivaji Science College
Amravati (M.S)- 444603, India
[2,5]Department of Physics, Dr. Ambedkar College, Deekshabhoomi
Nagpur (M. S.)- 440010, India
E-mail: sarkariresearch@gmail.com

Received 25 May 2020; accepted 12 September 2020

ABSTRACT

Substituted M-type calcium hexaferrite, $Ca(CoSn)_xFe_{(12-2x)}O_{19}$, as a function of doping rate (x=1,3,4) was synthesized by sol-gel method. The X-Ray diffraction reveals that the crystal has hexagonal symmetry with space group P63/mmc (No.194) with two formula units per unit cell. Transmission Electron Microscope (TEM) studies affirmed the particle size in nanometer range. The Vibrating Sample Magnetometer (VSM) studies of the as grown samples suggested that the saturation magnetization (M_s) increases with substitution. It was also found that the parameters Hc, Tc and SQR were known to decrease with doping degree.

Keywords: XRD, TEM, VSM, Magnetic Studies

1. Introduction

Hexaferrites are a special class of magnetic oxides characterized by many favorable physical and chemical properties. Since their discovery in the 1950s, a great deal of research work has focused on their synthesis and the modification of their properties [1-4]. Because of their high efficiency, low cost and small volume, hexaferrites find wide applications in numerous fields. Many new magnetic microwave devices (radar electronics, wireless technologies, phase shifters, data storage, active responsive components, sensors and transducers) are envisioned using planar, self-biased, and low loss hexaferrite materials. [5-9]. Ch. Mamata et al. [10] reports that the enhanced resistivity of doped calcium hexaferrite is suitable for device application. Since the discovery of M-type hexagonal ferrites, extensive research has been carried out to improve their magnetic properties, particularly by the use of cationic substitutions [11,12]. The motive to bring out sizable volume of information about the applicability and viability of such samples for the development of modern sciences and technology has geared up the objective of this research work. From the literature survey we found that Calcium has not been much explored as a host material. Calcium is richer than strontium and barium on the earth. Therefore, M-type Calcium hexaferrite could be a suitable candidate material for low cost permanent magnet [13]. The dopants Co^{+2} and Sn^{+4} have better intrinsic magnetic properties than Fe^{+3}. Moreover, the ionic radii of the dopants are comparable to the host material. Also both the dopants come under high ferromagnetic materials.

2. Materials and method

The samples of M-type substituted hexaferrites with molecular formula $Ca(Co\text{-}Sn)_xFe_{12-2x}O_{19}$ were synthesized by changing the values of x=1,3,4. The reactive nitrates such as $Ca(NO_3)_2$, $Fe(NO_3)_3.9H_2O.Co(NO_3)_2.6H_2O$ and $SnCl_4$ as precursors were dissolved into de-ionized triple filtered distilled water at a temperature of 50°C for a period of 15-20 min. Fuels like glycine and urea were used as reducing agents to supply requisite energy to initiate exothermic reaction among the oxidants. The sol-gel was produced by dissolving precursors in unionized water in a conical flask. Then this gel was stirred for 15-20 minutes using a magnetic stirrer. This gel was further made more homogenous under the influence of simultaneous effect of heat and rotational energy. This was carried out for about 20-30 minutes till complete homogeneous thick gel was produced. This gel was then allowed to burn in a microwave oven which was digitally programmed to produce 'as-burned-sample'. This 'as-burned-sample' was kept rotating but without any exposure of microwave to cool it and to get out all the fumes from it. The ash of the sample was then grinded for 4 hours each in three cycles using pestle and mortar to make it more fine and ultrafine in order to produce nano hexaferrites. Phase identification and determination of lattice parameters were carried out by powder X-ray diffraction (XRD). Particle size was determined using Transmission Electron Microscope (TEM). Magnetic properties were discussed by magnetization measurements by measuring of B-H curve with vibrating sample magnetometer (VSM).

3. Results and discussion

3.1. X-Ray diffraction study

The X-Ray Diffraction spectrum of all samples was carried out and studied (Figure 1a). The crystalline phase characterization of the samples was carried out by a computer interfaced X-ray Diffractometer (PW-1710 PHILIPS, Holland) operating at 42.5 KV and 18.00 mA with Cu-Kα radiation. The diffraction was measured in the range from 20° to 80° with a step of 0.02°/second. The JCPDS files No. 27-1029 taken into consideration to verify crystalline structure of Co-Sn doped calcium Hexaferrites. The analysis revealed that in all the patterns the main peaks correspond to the hexagonal M-type phase with space group P63/mmc (No.:194). The existence of the most prominent planes (1 0 7) in our samples further reinstates the M-type hexagonal crystal structure. But a few weaker peaks are also observed and it is attributed that they correspond to hematite Fe_2O_3 family and $CaFe_2O_4$ phases. It is observed that the intensity of these peaks was found to increase with the increase in substitution degree, due to occupation of lattice sites by substituted ions. The high intense peak (107) is shifting toward lower Bragg angle as an increase of Co–Sn substitution (x) as shown in Fig.1 (b). This may be due to the larger ionic radii of Sn^{4+} (0.71Å) and Co^{2+} (0.745 Å) compared to Fe^{3+} (0.645 Å) cations. It is clear from Fig.1 (b) that the relative intensity of the peaks changes may be due to some distortion in the crystal structure after Co–Sn substitution. From structural parameters it is evident that lattice constant 'a' reflects less variation while 'c' initially varies rapidly and again decreases with the substitution (Table 1). This is in agreement with the fact that all hexagonal types exhibit constant lattice parameter 'a' and variable parameter 'c' but having a bit of variation as reported by Kojima et al [14]. It also indicates that change in easy magnetized c-axis is larger than that in a-axis with Co^{2+} and Sn^{4+} ion substitution. This is attributed due to large ionic radii of Co^{2+} ion (0.72 Å) and Sn^{4+} ion (0.71 Å) than Fe^{3+} ion (0.64 Å). These

observations resemble with those reported independently by Gonzalez Angeles [15-18]. The change in lattice constants also varies with the distance between magnetic ions resulting in the change of exchange interaction and thus magnetic properties are altered with the substitution degree.

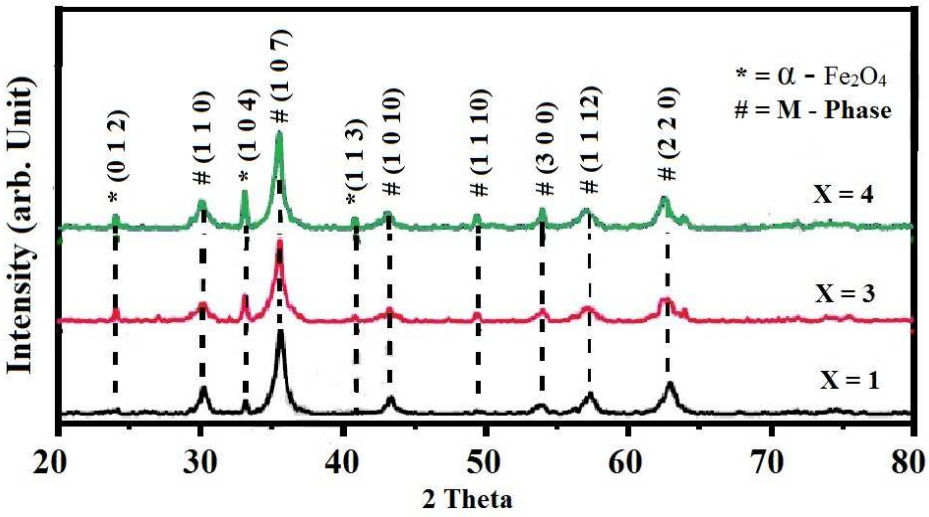

Figure 1: (a) X-ray diffraction patterns of $Ca(Co\text{-}Sn)_xFe_{12-2x}O_{19}$ (x = 1, 3, 4)

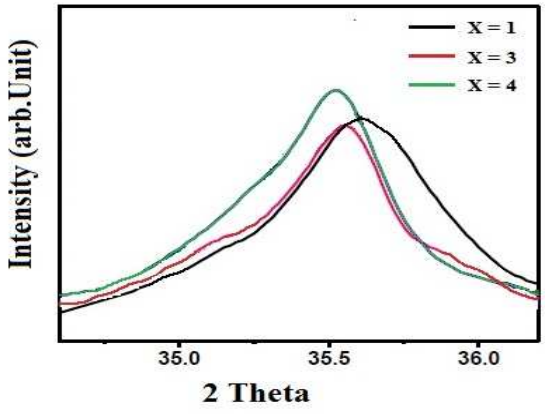

Figure 1: (b) Enlarged view of the (107) Bragg peak

Table 1: Structural and Morphological Properties of Samples

Sr. No.	Chemical Formula of Sample	Lattice Parameter		Axial Ratio	Crystallite Size D	Volume V	Bulk Density D_b	X–Ray Density D_x	Porosity P
		a	C						
		(Å)	(Å)		(nm)	$(Å)^3$	(gm/cm^3) ±0.01	(gm/cm^3) ±0.01	(%)
1	$Ca(Co\text{-}Sn)Fe_{10}O_{19}$	5.8247	22.0793	3.7906	17.831	648.72	4.981	5.5290	9.9121
2	$Ca(Co\text{-}Sn)_3Fe_6O_{19}$	5.8503	22.3116	3.8138	23.446	661.32	5.644	6.0859	7.262
3	$Ca(Co\text{-}Sn)_4Fe_4O_{19}$	5.8584	22.2156	3.7921	31.789	660.30	5.989	6.4270	6.815

3.2. Morphological study

The Particle size was confirmed by TEM studies (Figure 2). The TEM of the samples was carried out by the instrument of make PHILIPS, Model CM 200 having operating voltage 20-200 KV and resolution 2.4 Å. The TEM studies reveal that Co-Sn doped Calcium Ferrite particles are hexagonal platelets with a homogenous distribution and improved X-ray and Bulk density. As shown in Figure 2, the electron diffraction pattern shows ring patterns superimposed with spots. It reveals the poly-crystallinity of individual crystallites and also confirms the formation of the calcium hexaferrite phase as reported by Fu et al. [19]. The average particle size of nano particles produced is measured to be around 11.52 nm based on the TEM studies. As shown in Figure 2, thin plates of nearly hexagonal shape are formed exactly as obtained by Rosler et al. [20]. Also, from the Debye-Scherrer formula the average particle size was counter verified to be ≈ 0.94 nm.

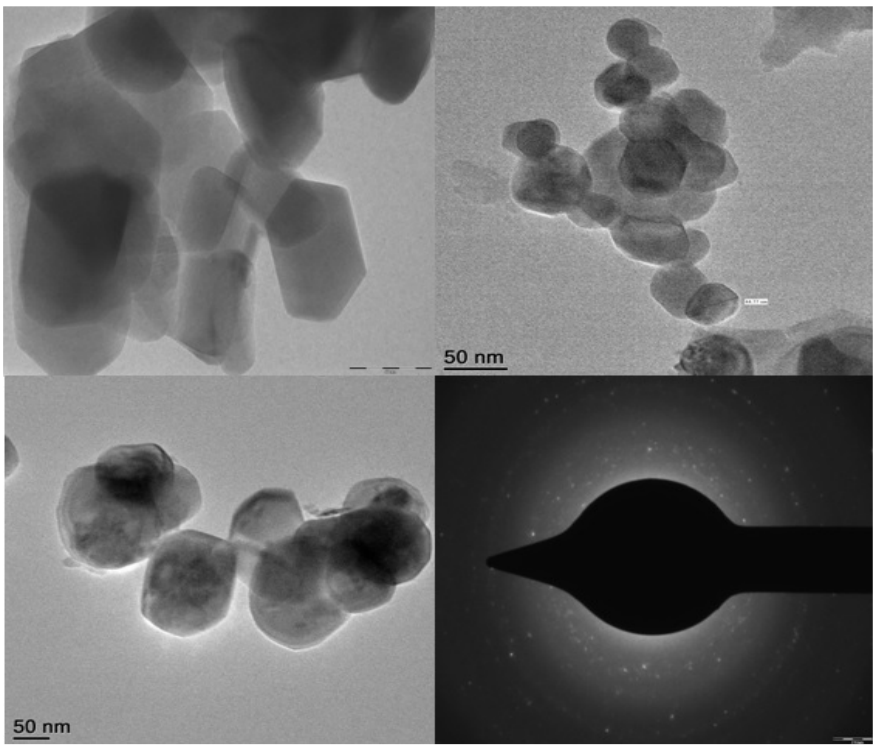

Figure 2: Magnified view of transverse electron micrograph with electron diffraction pattern in an inset

3.3. Magnetic study

Magnetization measurements of the samples were carried out using a fully Integrated Vibrating Sample Magnetometer (Lake Shore 7400) at room temperature with an applied magnetic field of 20 KG to reach saturation values. It is having configuration of 1×10^{-7} emu noise floor at10 s/pt and 7.5×10^{-7} emu noise floor at 0.1 s/pt. It provides sufficient field strength to get sample saturated. The used system was the most sensitive electromagnet-based VSM's commercially available and was having the broadest temperature range capability of 4.2 K to 1273 K (– 269 °C to 1000 °C). The B-H curves (Figure 3(a), 3(b), 3(c)) of the samples reveal that Co-Sn substituted Calcium Hexaferrite samples exhibit sharp increase in magnetization at low applied field which slows down at high field. There is a large reduction in hysteresis with substitution. It is observed that the doped samples nearly get into saturated state. The occurrence of this state is due to large drop in anisotropy field as shown in variation of coercivity (HC). The Co-Sn substituted calcium hexaferrites powders have a very different set of magnetic properties as listed in Table 2. The table shows that the saturation magnetization (Ms) increases from 11.5038 emu/g to 24.5117emu/g and further decreases to 17.7815 emu/g with substitution. The saturation magnetization Ms increasing with Co-Sn ions substitution could have happened because of the replacement of Fe^{3+} ions in spin up state by Co^{2+} and Sn^{4+} ions. The magnetic moments of both ions are not able to cancel out with spin down moments of Fe^{3+} ions, thereby decreasing Ms.

It has been observed the coercivity Hc of doped samples decreases with substitution of Co^{2+} and Sn^{4+} ions. This frequent reduction in anisotropy is primarily related to intrinsic effect associated with replacement of Fe^{3+} ions at both 4f2 and 2b sites. These two sites contribute to large anisotropy field as reported by Mendoza-Suarez et al. [21]. Another factor responsible for the decrease in coercivity is extrinsic effect accompanied by increase in grain size with substitution as depicted in TEM morphology of the samples. The fall in coercivity is an indication of soft ferrite behavior. Similar trend has also been observed by Ghasemi et al [22] in other hexagonal ferrite. From Table 2, it is clear that the Curie temperature (Tc) of the sample decreases with Co^{2+} and Sn^{4+} ions substitution. This can be explained on the basis of number of magnetic ions present in the two sub-lattice and their mutual interactions. As the Fe3+ ions are replaced by Co^{2+} and Sn^{4+} ions with low magnetic moment, the number of magnetic ions decreases on both sides weakening AB super-exchange interaction of type FeA^{3+}–O–FeB^{3+}.This eventually imbalances the spin alignment at lower thermal energy, leading to decrease in Curie temperature (Tc). Similar reduction of Tc with substitution has also been observed in Ba-Cr hexagonal ferrites by Kim et al. and by Xiannsong Liu et al. [23] in Sr-La hexagonal ferrites. Also as reported by Litsardakis et al. [24-26], Fe/Co or Fe/Sn weakens the exchange interaction and hence it reduces the Curie point.

Variation of magnetization as a function of temperature were mentioned in the figure 4 the curie temperature of the prepared material were found to be 659.30K, 544.59K and 465.97K for sample-1($Ca(Co\text{-}Sn)Fe_{10}O_{19}$) sample-2 ($Ca(Co\text{-}Sn)_3Fe_6O_{19}$) and sample-3 ($Ca(Co\text{-}Sn)_4Fe_4O_{19}$) respectively. From the figure 4 it has been observed that the Curie temperature goes on decrease with decreasing the concentration of Fe^{3+} ion, this is due to the fact of magnetic interaction between Fe^{3+} ions and other cation. In the M-type hexaferrite Fe^{3+} cation accommodates at three different types of interstitial cationic positions: tetrahedral, octahedral and bipyramidal. Similarly Co^{2+} cation occupied at octahedral and tetrahedral position but with opposite spin of Fe^{3+} cation which may be the reason for cancelation of magnetization of the material with increasing the concentration of Fe^{3+} ion. Here the magnetization value for sample-1is greater than sample -2 and sample -3, therefore sample -1 has highly oriented magnetic moments and it needs the large amount of heat to disorient, hence Tc (Curie temperature) is more for the sample -1 as compare to other two samples as mentioned in figure 4.

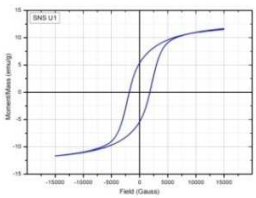

Figure 3 (a)

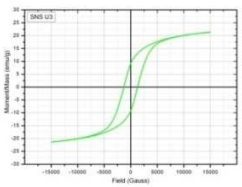

Figure 3 (b)

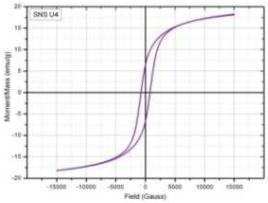

Figure 3 (c)

Figure 3: Hysteresis loop for sample 1, 2 and 3

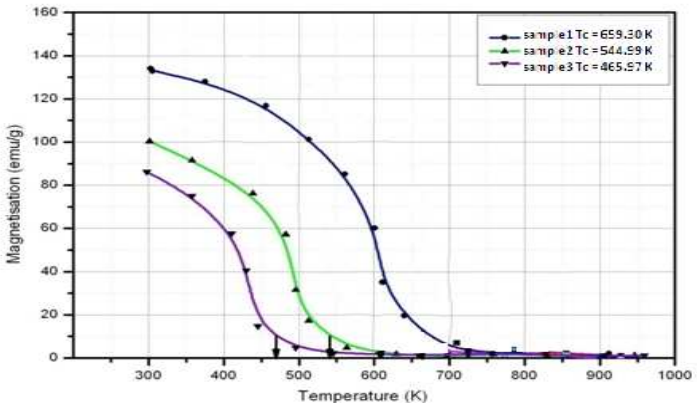

Figure 4: Magnetization as a function of temperature

Table 2: Magnetic properties of samples

Name of Sample	Doping Degree X	Chemical Formula for the Sample	M_s	M_r	SQR	H_c	T_c
			emu/g	emu/g		G	K
Sample 1	1	Ca(Co-Sn)$Fe_{10}O_{19}$	11.5038	5.37827	0.4675	1799.02	659.30
Sample 2	3	Ca(Co-Sn)$_3Fe_6O_{19}$	24.5117	9.2029	0.3754	1196.49	544.99
Sample 3	4	Ca(Co-Sn)$_4Fe_4O_{19}$	17.7815	6.54563	0.3681	603.12	465.97

3.4. Temperature dependence of susceptibility

The temperature dependence of the magnetic susceptibility was carried out by the bridge method, where the samples were heated at a constant rate of 4°C /min. The graphical variation of the magnetic susceptibility versus temperature is as shown in the Figure 5. The temperature dependence of magnetic susceptibility measurement (Figure 5) showed that the decrease of the magnetic ordering temperature with dopant level is less rapid which allows applications of Co-Sn doped M-type ferrites at higher temperature. Because of difference in the magnetic moment of Co^{2+} and Fe^{3+} ions a ferromagnetic behavior is achieved by the samples. This dependence shows that in the vicinity of the Curie temperature, there appears a sharp Hopkinson peak for single phase M-hexaferrite. These Hopkinson peaks are found to be broadened and their peak values fall with rising x. This is attributed mainly to a distribution in the shape of the particles and a spread in the composition.

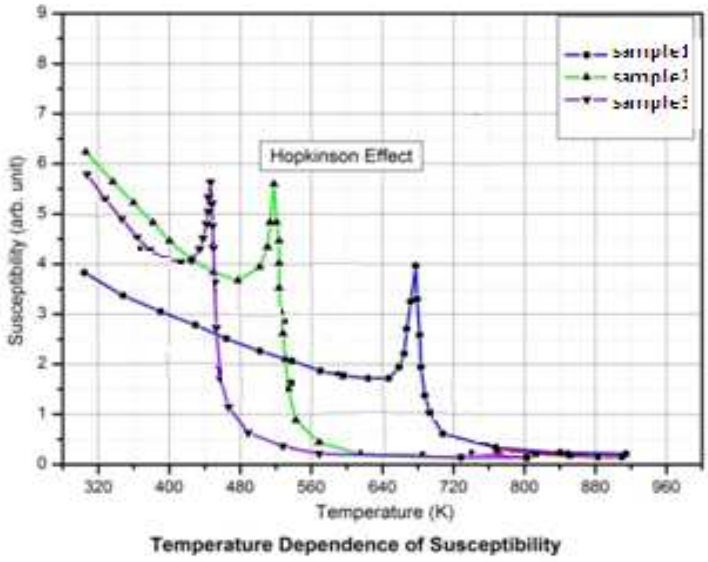

Figure 5: Temperature dependence of susceptibility

The canting is not worked out in this case but the observed result shows at low temperature, canting and A–B interaction play a complex role such that almost a feeble magnetic antiferrimagnetic exchange is involved and hence a lesser degree of curvature is observed in the present case. The high value of Tc (659.30 K) demonstrates that some inter-sublattice exchange interactions are formed. Moreover in hexaferrites the interaction between two close sites, such as 2a-12K, 2a-4f1 and 2b-12K is decisive for strong magnetic character as quoted by Turilli et al. [27] and Van Uitert [28]. Whenever magnetic ions i.e. Co^{2+} and Fe^{3+} are present in these sites, strengthening of super-exchange interaction produces an increase in the magnetic characteristics such as Curie temperature, magnetization, etc. All these findings are supported by the research work carried out by V. M. Nanoti et al. [29–30] as predicted by Stoner-Wohlfarth model [31, 32], the SQR should be less than 0.5 for the single domain magnetic structure of the samples. In our case, all the samples have SQR close to and less than 0.5 which eventually confirms the single domain structure of the samples. The temperature dependence of magnetic susceptibility measurement showed that the decrease of the magnetic ordering temperature with dopant level is less rapid which allows applications of Co-Sn doped M-type ferrites at higher temperature. Because of difference in the magnetic moment of Co^{2+} and Fe^{3+} ions a ferromagnetic behavior is achieved by the samples. The introduction of Co^{2+} ions into the tetrahedral sites would not change the net magnetization of materials but the replacement of Sn^{4+} ions into the octahedral sites must have caused the variation in the net magnetization of materials. According to the variation of the saturation magnetization of the series $Ca(Co\text{-}Sn)_xFe_{12-2x}O_{19}$ with x (as represented in the Table 2), we conclude that the increase of the net magnetizations of materials for x = 3 and 4 can be attributed due to the replacement of diamagnetic Sn4+ ions into the spin down sublattices 4f2. When x > 3.0; Sn^{4+} ions

substitute for the spin-down sublattices (4f2) and other octahedral spin-up sublattices (12K, 2a, 2b); therefore, the values of saturation magnetization of compounds decreases with x and the magnetic collinearity of materials also decrease gradually as explained by Slama et al. [33].

4. Conclusion

Co-Sn doped nanoscale Calcium Hexaferrites were synthesized using Sol-Gel method. It was observed from the intensity peaks in the XRD patterns that as the doping concentration increases, other intermediate phase like hematite α-Fe_2O_3 gets lowered. The TEM studies revealed that Co-Sn doped Calcium Ferrite particles are hexagonal platelets with a homogenous distribution and improved X-ray and Bulk density. It has been observed that the coercivity of doped samples decreases with substitution of Co^{2+} and Sn^{4+} ions. This frequent reduction in anisotropy was attributed to intrinsic effect associated with replacement of Fe^{3+} ions at both 4f2 and 2b sites. The deviation in the magnetic properties of the samples was attributed to the change from a single-domain to a multi-domain structure which was led by agglomeration. The saturation magnetization Ms increasing with Co-Sn ions substitution could be a result of the replacement of Fe^{3+} ions in spin up state by Co^{2+} and Sn^{4+} ions.

Acknowledgement. Dr. N. N Sarkar acknowledges to the Department of Physics of Shri Shivaji Science College Amravati and Dr. Ambedkar College, Deekshabhoomi, Nagpur for extending their support to carryout research work.

REFERENCES

1. R.C. Pullar, A review of the synthesis, properties and applications of hexaferrite ceramics, Prog. Material Science, 57 (2012) 119-133.
2. Z. Chen, A. Yang, C. Xie, Q. Yang, C. Vittoria, V.G. Harris, High-rate reactive ion etching of barium hexaferrite films using optimal CHF_3/SF_6 gas mixtures, Appl. Phys. Lett., 94 (2009) 112-118.
3. N.T.Tayade, Perspective of distortion and vulnerability in structure by using the CdS-ZnS composite, Journal of Physical Sciences, 22 (2017) 137-150.
4. E.S. Alhwaitat, S.H. Mahmood, M. Al-Hussein, O.E. Mohsen, Y. Maswadeh, I. Bsoul, A. Hammoudeh, Effects of synthesis route of the structural and magnetic properties of $Ba_3Zn_2Fe_{24}O_{41}(Zn_2Z)$ nanocrystalline hexaferrites, Ceram. Int., 44 (2018) 779-787.
5. M.Wang, Preparation of pure iron/Ni–Zn ferrite high strength soft magnetic composite by spark plasma sintering, Journal of Magnetic Material, 361 (2014) 166–169.
6. A.B. Salunkhe, V.M. Khot, M.R. Phadatare, N.D. Thorat, R.S Joshib, H. M. Yadav, S.H.Pawar, Low temperature combustion synthesis and magnetostructural properties of Co–Mn nanoferrites, Journal of Magnetism and Magnetic Materials, 352 (2014) 91–98.
7. A.A. Mirghni, M.A. Siddig and M. Ibrahim, Synthesis of $Zn_{0.5}Co_xMg_{0.5-x}Fe_2O_4$ nano-ferrites using co-precipitation method and its structural and optical properties, American Journal of Nano Research and Applications, 3 (2015) 27-32.

8. S.M. Rathod, V.G. Deonikar, R.R. Shah and P.P. Mirage, Synthesis, magnetic and optical properties of $Ni_{0.5}Co_{0.5}Al$ nanoferrite by autocombustion technique, International Journal of Engineering Research & Technology, 3 (2014) 115-119.
9. Erum Pervaiz, I. H. Cul, Low temperature synthesis and enhanced electrical properties by substitution of Al^{3+} and Cr^{3+} in Co-Ni Nanoferrites, Journal of Magnetism and Magnetic Materials, 343 (2013) 194-202.
10. Ch. Mamata, M. Krisnaiha, C.S.Prakash, K. Rewatkar, structural and electrical properties of aluminium substituted nano calcium ferrites, Procedia Materials Science, 5 (2014) 780 – 786.
11. N.N. Sarkar, Soft Ferrite: A brief review on structural, magnetic behavior of nanosize spinel ferrites, Material Research Foundation, 31 (2018) 237-260.
12. B.D. Cullity, Elements of X-Ray Diffraction. Addison-Wesley Publishing Company, 1 (1956) 333-340.
13. T. Kikuchi, T. Nakamura, T. Yamasaki, M. Nakanishi, Synthesis of La-Co substituted m-type calcium hexaferrite by polymerizable complex method, Materials Science and Engineering, 18 (2011) 255-260.
14. A. Zubair, Structural, morphological and magnetic properties of Eu-doped $CoFe_2O_4$ nano-ferrites, Results Physics, 7 (2017) 3203-3208.
15. Gonzalez-Angeles, G. Mendoza-Suarez, A. Gruskova, M. Papanova, J. Slama, Magnetic studies of Zn-Ti-substituted barium hexaferrites prepared by mechanical milling, Materials Letters, 59 (2005) 26–31.
16. D. Limin, H. Zhidong, Z. Yaoming, Wu Ze and Z. Xianyou, Synthesis of hexagonal barium ferrite nanoparticle by Sol-Gel method, Journal of Rare Metals, 25 (2006) 605-610.
17. Simon Thompson, Neil J. Shirtcliffe, Eoin S. O'Keefe, Steve Appleton, Carole C. Perry, Synthesis of $SrCo_xTi_xFe_{(12-2x)}O_{19}$ through sol–gel auto-ignition and its characterization, Journal of Magnetism and Magnetic Materials, 292 (2005) 100–107.
18. N.N.Sarkar, Structural and magnetic study of Zr^{4+} substituted magnesium ferrite nano-particles, Journal of Physical Sciences, 22 (2017) 107-113.
19. Yen Pei Fu, Cheng-Hsiung Lin, Ko-Ying Pan, Strontium hexaferrite powders prepared by a microwave-induced combustion process and some of their properties, Journal of Alloys and Compounds, 349 (2003) 228–231.
20. S. Rosler, P. Wartewig, H. Langbein, Synthesis and characterization of hexagonal ferrites $BaFe_{12-2x}Zn_xTi_xO_{19}$ ($0 \leq x \leq 2$) by thermal decomposition of freeze-dried precursors, Crystal Research and Technology 38(2003) 927–934.
21. Mendoza Suarez G, Rivas–Vaquez L P, Corral–Huacuz J C, Fuentes, Escalante–Garcia A F, Magnetic properties and microstructure of $BaFe_{11.6-2x}Ti_xM_xO_{19}$ (M= Co, Zn, Sn) compounds, Journal of Condensed Matter, 339 (2003) 110–118.
22. A. Ghasemi, A. Hossienpour, A. Morisako, Saatchi, M. Salehi, Electromagnetic properties and microwave absorbing characteristics of doped barium hexaferrite, Journal of Magnetism and Magnetic Materials, 302 (2006) 429–435.
23. Xiansong Liu, Wei Zhong, Sen Yang, Zhi Yu, Ben Xi Gu, Youwei Du, Influences of La^{3+} substitution on the structure and magnetic properties of M-type strontium ferrites, Journal of Magnetism and Magnetic Materials, 238 (2002) 207–214.

24. G. Litsardakis, I. Manolakis, C. Serletis, K.G. Efthimiadis, Effects of Gd substitution on the structural and magnetic properties of strontium hexaferrites, Journal of Magnetism and Magnetic Materials, 316 (2007) 170–173.
25. J. Huang, H. Zhuang, W.L. Li, Synthesis and characterization of nano crystalline BaFe12O19 powders by low temperature combustion, Materials Research Bulletin, 38 (2003) 149–159.
26. Kishor Rewatkar, Vivek Nanoti, Structural and magnetic behavioral improvisation of nanocalcium hexaferrites**,** Materials Science and Engineering B, 168 (2010) 156-160.
27. G. Turilli, F. Licci, S. Rinaldi, A. Deriu, Mn^{2+}, Ti^{4+} substituted barium ferrite, Journal of Magnetic Materials, 59 (1986) 127-133.
28. L G Van Uitert, Magnetic induction and coercive force data on members of the series $BaAl_xFe_{12-x}O_{19}$ and related oxides, Journal of Applied Physics, 28(1957) 317-322.
29. V. M. Nanoti, D.K. Kulkarni, Crystallographic transport and magnetic studies of Cr-substituted Zn-Co ferrites, Materials Letters, 33 (1997) 37–39.
30. V. M. Nanoti, C. S. Prakash, D.K. Kulkarni, Magnetic behaviour of Cr-substituted Zn-Cu ferrites, Materials Letters, 24 (1995) 167–169.
31. E. C. Stoner, E. P. Wohlfarth, A mechanism of magnetic hysteresis in heterogeneous alloys, Philosophical Transactions of the Royal Society A Mathematical, Physical and Engineering Sciences. 240 (1948) 599- 642.
32. E.P. Wohlfarth, Relations between different modes of acquisition of the remnant magnetization of ferromagnetic particles, Journal of Applied Physics, 29(1958) 595-610.
33. J. Slama, A. Gruskova M. Papanova, D. Kevicka, R. Dosoudil, V. Jancarik, A. Gonzalez, G. Mendoza, Magnetic properties of Me-Zr substituted Ba-hexaferrite, Journal of Magnetic Materials, 272 (2004) 385-393.